Analytica Chimica Acta 988 (2017) 34–40

Contents lists available at ScienceDirect

Analytica Chimica Acta

journal homepage: www.elsevier.com/locate/aca

Improved analytical techniques of sulfur isotopic composition in nanomole quantities by MC-ICP-MS

Tsai-Luen Yu [a, b, 1], Bo-Shian Wang [c, 1], Chuan-Chou Shen [a, b, *], Pei-Ling Wang [d], Tsanyao Frank Yang [b], George S. Burr [e], Yue-Gau Chen [b]

[a] High-Precision Mass Spectrometry and Environment Change Laboratory (HISPEC), Department of Geosciences, National Taiwan University, Taipei 10617, Taiwan, ROC
[b] Department of Geosciences, National Taiwan University, Taipei 10617, Taiwan, ROC
[c] Taiwan Ocean Research Institute, National Applied Research Laboratories, Kaohsiung 80424, Taiwan
[d] Institute of Oceanography, National Taiwan University, Taipei 10617, Taiwan, ROC
[e] Department of Oceanography, National Sun Yat-sen University, Kaohsiung 80424, Taiwan, ROC

HIGHLIGHTS

- Accurate analysis of $\delta^{34}S$ and $\Delta^{33}S$ with 2 SD precision of ±0.18‰ and ±0.10‰ by using 3 nmol S.
- Quantification of S losses during sample pretreatment and membrane desolvation.
- Improved S memory reduction and blank evaluation by adding adequate Na to the washing solution.
- Successful application to low-S marine sediment pore fluids.

GRAPHICAL ABSTRACT

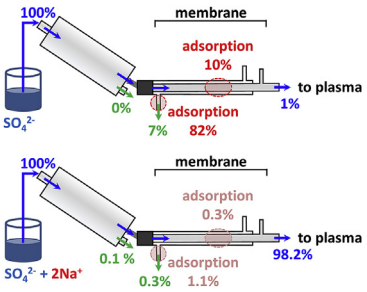

ARTICLE INFO

Article history:
Received 16 May 2017
Received in revised form
2 August 2017
Accepted 7 August 2017
Available online 18 August 2017

Keywords:
Sulfur isotopes
MC-ICP-MS
Desolvation
Sodium

ABSTRACT

We propose an improved method for precise sulfur isotopic measurements by multi-collector inductively coupled plasma mass spectrometry (MC-ICP-MS) in conjunction with a membrane desolvation nebulization system. The problems of sulfur loss through the membrane desolvation apparatus are carefully quantified and resolved. The method overcomes low intrinsic sulfur transmission through the instrument, which was initially 1% when operating at a desolvation temperature of 160 °C. Sulfur loss through the membrane desolvation apparatus was resolved by doping with sodium. A Na/S ratio of 2 mol mol^{-1} produced sulfur transmissions with 98% recovery. Samples of 3 nmol (100 ng) sulfur achieved an external precision of ±0.18‰ (2 SD) for $\delta^{34}S$ and ±0.10‰ (2 SD) for $\Delta^{33}S$ (uppercase delta expresses the extent of mass-independent isotopic fractionation). Measurements made on certified reference materials and in-house standards demonstrate analytical accuracy and reproducibility. We applied the method to examine microbial-induced sulfur transformation in marine sediment pore waters from the sulfate-methane transition zone. The technique is quite versatile, and can be applied to a range of materials, including natural waters and minerals.

* Corresponding author. High-Precision Mass Spectrometry and Environment Change Laboratory (HISPEC), Department of Geosciences, National Taiwan University, Taipei 10617, Taiwan, ROC.
E-mail address: river@ntu.edu.tw (C.-C. Shen).
[1] T.-S. Yu and B.-S. Wang contributed equally to the work.

http://dx.doi.org/10.1016/j.aca.2017.08.012
0003-2670/

1. Introduction

Sulfur isotope geochemistry has been applied widely in geological and environmental studies. The relatively large isotopic fractionation between the two principal nuclides, ^{32}S and ^{34}S, for example, has been used to understand Earth's lithosphere, hydrosphere, atmosphere, and biosphere [1,2]. In recent years, the less abundant nuclides, ^{33}S and ^{36}S, have also been used in geologic applications spanning the past four billion years [3]. In the marine system, the biogeochemical cycles of sulfur involve algal photosynthesis, protein synthesis, and microbial metabolism [4–6]. These pathways can be distinguished using sulfur isotope ratios [6]. Microbial mineralization causes large sulfur isotopic fractionation through sulfate reduction and anaerobic oxidation of methane (AOM) [7–9]. Both sulfate reduction and methane oxidation transform sulfate into various sulfide species of H_2S, HS^- and S^{2-} and ultimately deplete dissolved sulfate concentrations to sub-micromolar levels [10,11]. This concentration range, combined with the limited volume of pore fluid that can be conveniently collected, restrict the use of conventional gas source mass spectrometric approaches for analysis [12–14].

Double spike thermal ionization mass spectrometry (DS-TIMS) is capable of sulfur isotopic analysis for very small sample size, down to 6.25 nmol S [15,16]. The requisite tedious sample loading and instrumental operation, however, serve to limit sample throughput. Single particle-mineral sulfur isotopic analysis can be achieved by Nanoscale Secondary Ion Mass Spectrometry with dimensions down to submicron scale and nanogram-size sulfur [17]; yet, a sacrifice in analytical precision is inevitable. Alternatively, sector field inductively coupled plasma mass spectrometry (SF-ICP-MS), with high overall sensitivity detected by single collector, provides a one standard-deviation (SD) reproducibility of ±0.4‰ for $^{34}S/^{32}S$ using 3.1 nmol S and medium resolution [18]. The relatively simple sample preparation and high analytical throughput provide an advantage in experimental efficiency. Recent developments in multi-collector ICP-MS (MC-ICP-MS) in combination with improved inlet system for water and solid samples further improved reproducibility to ±0.2–1‰ (2 SD) [19–23]. Instrumental mass bias can be corrected for by either standard-sample-standard bracketing (SSB) [24] or by external normalization using silicon doping [20] to achieve accurate sulfur isotope ratios.

In the ICP, extremely high $^{16}O^{16}O^+$ interferences on $^{32}S^+$ observed in the stable inlet system (i.e., wet plasma) can be effectively decreased through sample desolvation (i.e., dry plasma). However, previous attempts showed that sulfur transmissions decline considerably in a desolvation system when injecting dilute pure sulfuric acid [20]. Several studies have reported methods of improving sulfur transmission through membrane desolvation [25–28]; however, the detailed mechanism of sulfur loss was still unknown.

To understand the factors causing the sulfur signal loss in a dry-plasma system and optimize instrumental conditions, an evaporation experiment was first carried out to clarify the effect of heating temperature on dissolved sulfate volatility. The effects of desolvation-induced sulfur loss and sodium addition was quantitatively addressed. Sulfur transfer efficiency and stability were improved. The resulting analytical techniques were successfully used to investigate sulfur isotopic features in low-sulfur marine pore fluids offshore southwestern Taiwan.

2. Methods

2.1. Experimental setup

Chemistry and instrumental analyses were conducted at the High-Precision Mass Spectrometry and Environment Change Laboratory (HISPEC), National Taiwan University. Chemical procedures were performed in a class-10,000 geochemical clean room with class-100 (actually achieves class-10) positive pressure laminar flow benches. Ultrapure hydrochloric acid (HCl) and nitric acid (HNO_3) (ULTREX II grade), purchased from J.T. Baker Chemical Co., were diluted to appropriate concentrations with ultrapure water (Millipore Milli-Q Academic and Milli-Q Element) [29]. All plastic containers, including Teflon vials and bottles, were acid-cleaned.

Sulfur concentration was determined on a SF-ICP-MS, Thermo Fisher Scientific ELEMENT 2, coupled with a typical wet introduction system using a Scott-type double-pass spray chamber. Sulfur isotopic composition was analyzed on a MC-ICP-MS, Thermo Fisher Scientific NEPTUNE. Both sample introduction techniques of wet plasma with a Scott-type double-pass spray chamber and dry plasma with a membrane desolvation nebulization device, Cetac ARIDUS I or II, were used.

Mono-elemental sulfur (High-Purity Standard HP-S and SPEX ICP-MS Standard SPEX-S, 10000 and 1000 mg L^{-1}) and sodium solution (High-Purity Standard, 1000 mg L^{-1}) were diluted to 0.1–9 μmol L^{-1} S, respectively, and 0.2–18 μmol L^{-1} Na with 0.25 mol L^{-1} HNO_3 as working standards. The solution with 0.25 mol L^{-1} HNO_3 + 6.3 μmol L^{-1} Na was used for routine sodium additive to purified sulfur aliquots before instrumental analysis. Three reference silver sulfides IAEA-S-1, IAEA-S-2 and IAEA-S-3, reference seawater NASS-5, and one of anomalous mass independent sulfur isotope fractionation in Archean sulfide [30,31] were used to validate the chemical and analytical procedures.

Thirteen pore fluids, 0.5–1 mL, were extruded at intervals of 20 cm and then extracted with 0.45-μm filter onboard at depths of 0–252 cm of a marine sediment core, collected on March 11–18, 2013, offshore southwestern Taiwan (21°47.172′N, 119°42.683′E). The unacidified samples were used for the determination of sulfate concentration analyzed by ion chromatography with analytical precision of ±4% (2 SD) [32]. Acidified 10 μL aliquots with 7 mol L^{-1} HNO_3 were used for sulfur isotopic measurement.

Silver sulfide samples, 10 mg each, were digested in a 2 mL HCl-HNO_3 solution (1:1 wt %) on a hot plate at 70 °C. Digested reference materials, seawater and pore water samples were purified using an AG1-X8 anion exchange resin. The column procedure, using a PFA mini-column (I.D. = 2 mm), was modified from Menegário et al. [33]. Typical sulfur recovery yield was >97%. Sulfur blanks in reagents, including water, diluted nitric acid, and sodium solution, were determined. Total sulfur blanks of column separation and overall procedure were analyzed.

2.2. Sulfur evaporation test

Potential sulfur loss during evaporation was examined on a hotplate, with different settings from 70 to 160 °C, for 10 min using aliquots of aqueous samples containing 16 μmol L^{-1} S in 0.25 mol L^{-1} HNO_3 with and without 32 μmol L^{-1} Na. For each set, a 2-μL aliquot was dripped onto a 15 mL PFA lid. The dried samples were dissolved and mixed with 0.5 mL 0.25 M HNO_3. Sulfur content was determined on a SF-ICP-MS.

2.3. Sulfur transmission evaluation

The effect of a membrane desolvation nebulization device, a Cetac ARIDUS I, was evaluated for the transformation of sulfur species and transmission efficiency. Two tested samples containing 3.1 mol L^{-1} S were prepared in 0.25 mol L^{-1} HNO_3, one of which contained 6.3 mol L^{-1} Na. The membrane desolvation device, with a sample Ar flow rate at 1 L min^{-1}, sweep Ar gas at 5 L min^{-1}, and N_2 gas at 7 mL min^{-1}, was warmed up without being connected to the ICP-MS. After a 2-h warm up, the system was initially washed with 0.25 mol L^{-1} HNO_3 for 10 min, followed by injecting a 3.1 mol L^{-1} S solution into the device for 30 min. Three 15 mL centrifuge tubes filled with 5 mL 4 mol L^{-1} NaOH were used to collect moisture and gas samples from three outlets, including sample out, sweep gas out, and drain, during injection. The system was then washed using 0.25 mol L^{-1} HNO_3 with 6.3 mol L^{-1} Na for 30 min, and the outflows were collected during washing. Afterward, a solution containing 3.1 mol L^{-1} S and 6.3 mol L^{-1} Na was introduced for 30 min, and the outflows were collected. The system was washed again for 30 min with 0.25 mol L^{-1} HNO_3 containing 6.3 mol L^{-1} Na, and the outflows were collected. Sulfur contents of all collected outflow samples, diluted with 0.25 mol L^{-1} HNO_3, were analyzed on SF-ICP-MS.

2.4. Instrumentation and sensitivity

The MC-ICP-MS was stabilized for at least one hour after the plasma was ignited. Instrumental settings, including torch position, nebulizer gas flow rate [34], source lenses, and zoom optics, were optimized. For the dry sample introduction system, sweep Ar gas and N_2 gas were set at 4.9–5.3 L min^{-1} and 5–9 mL min^{-1}, respectively. Typical settings are listed in Table 1.

Ion beam intensities of the isotopes, ^{32}S, ^{33}S, and ^{34}S, were detected with three Faraday cups at medium resolution ($M/\Delta M = 5000$). The lowest ^{36}S isotope was not detected due to significant isobaric $^{36}Ar^{+}$ interference. Cup configurations are presented in Table 1. Cup positions were shifted to the low-mass side by 0.3 atomic mass unit (amu) to avoid major O_2^{+} peaks [20]. The instrumental background was monitored before introducing a sample. Nine blocks of 10 integrations with 1.049 s duration for each cycle were selected, taking 3 min per sample measurement. After measuring each sample, the introduction system was cleaned with 0.25 mol L^{-1} HNO_3 doped with 0.31 μmol L^{-1} Na for 3 min to reduce the residual sulfur to less than 0.01% from previous analysis. An ion beam intensity of 3–5 V for ^{32}S was generated by a sulfur solution of 1 μmol L^{-1} at a sample uptake rate of ~60 μL min^{-1}. A 1-mL aliquot with 3 nmol S was routinely prepared for S isotopic analysis, yielding an intensity of 9–15 V for ^{32}S. Volume consumed was ~300 μL for each measurement. Quality control was checked daily before a routine SSB sequence. First, the Na-added blank (named 'BLK'), the reference standard IAEA-S-1 (named 'STD'), three reference standards, IAEA-S-2, IAEA-S-3, and NASS-5, and two working standards, HP-S and SPEX-S (named 'SMP'), were cross-checked following a "BLK-STD-SMP-STD-SMP-STD-BLK" sequence to assure the instrumental condition and analytical quality. Measurement of samples was carried out once the analytical precision and accuracy were verified.

Table 1
Operation parameters for MC-ICP-MS sulfur isotopic analysis.

Mass Spectrometer and Membrane Desolvator Setup	
Mass spectrometer setup	
MC-ICP-MS	Neptune (Thermo Fisher Scientific)
RF power	1200 W
Analyzer pressure	~2×10^{-9} mbar
Pt guard electrode	On, grounded
Sample cone	Jet (Ni)
Interface cone	X-skimmer (Ni)
Cooling gas	18 L min^{-1}
Auxiliary gas	1.0 to 1.1 L min^{-1}
Sample gas	0.7 to 1.0 L min^{-1}
Nebulizer	PFA-50 or PFA-100 (ESI)
Extraction lens	−640 to −595 V
Zoom optics	−2 to 0 V (Extraction Quad)
Cup configuration	C (32), H1 (33), H4 (34)
Resistors	C (10^{11} Ω), H1 (10^{12} Ω), H4 (10^{12} Ω)
Resolution	Medium
Membrane desolvator setup	
Desolvator	ARIDUS I or II
Sweep gas	4.9 to 5.3 L min^{-1}
Nitrogen gas	5 to 9 mL min^{-1}
Spray chamber (PFA) temperature	110 °C
Desolvator temperature	160 °C

2.5. Data reduction and quality control

An off-line data reduction was performed for spectral background correction, instrumental mass bias correction, and isotopic composition calculation. Calibrated isotope ratios are reported in lowercase and uppercase delta notation using the following two equations:

$$\delta^{x}S\ (‰) = \left\{ \left({}^{x}S/{}^{32}S \right)_{Sample} \Big/ \frac{1}{2}\left[\left({}^{x}S/{}^{32}S \right)_{Ref1} + \left({}^{x}S/{}^{32}S \right)_{Ref2} \right] - 1 \right\} \times 1000, \quad (1)$$

where x is 33 or 34, and the certified reference material IAEA-S-1 measured before (Ref1) and after (Ref2) the sample (Sample).

$$\Delta^{33}S(‰) = \left[\ln(\delta^{33}S/1000 + 1) - \lambda \times \ln(\delta^{34}S/1000 + 1) \right] \times 1000, \quad (2)$$

where λ is set to 0.515 defining the slope of $\delta^{33}S$ versus $\delta^{34}S$ via mass-dependent fractionation [35–37]. Uncertainties are calculated at 2 SD for external precision unless otherwise noted.

3. Results and discussion

3.1. Spectral interference and blanks

Isobaric interference can bias sulfur isotope measurement [21]. Evaluation of sulfur isotope ratios with and without spectral background correction is plotted in Fig. S1. Without background correction, a significant negative $\delta^{34}S$ offset of 0.8–1.5‰ is observed for 0.3–0.6 μmol L^{-1} S of reference material IAEA-S-2 from an acceptable range (Fig. S1), mainly caused by the low-mass tailing of $^{16}O^{16}O^{+}$ at 32 amu [21]. For sulfur contents >1.5 μmol L^{-1}, there is an absence of significant difference of all uncorrected and corrected sulfur isotopic data from certified ranges (Fig. S1).

Reagent blanks and procedural blanks are listed in Table S1. For reagents, sulfur blank is mainly from pure water, 7.2 nmol L^{-1}. Sulfur content in the sodium additive solution is 9.3 nmol L^{-1}, 77.4% from water, 20.4% from High-Purity Na 1000 mg L^{-1} standard, and 2.1% nitric acid. The contribution of overall procedural sulfur blank of 19 pmol is (1) 75% from column purification chemistry, (2) 25% from sodium additive and diluted nitric acid, and (3) 0.2–0.8% from introduction system of MC-ICP-MS (Table S1). This blank level is one order less than previous reports [25,27]. The total S blank, equivalent to 0.6% of sample S (3 nmol S in 1 mL 0.25 mol L^{-1}

HNO_3), accounts for maximum offsets of ±0.03‰ on both $\delta^{34}S$ and $\delta^{33}S$, only 1/6–1/5 of the external errors of S isotopic data.

3.2. Effect of temperature on sulfur vaporization

Nine sets of sulfur with and without sodium addition with different temperature values are plotted in Fig. 1. Without adding sodium, sulfur loss is not observed at temperatures ≦110 °C. Significant sulfur is lost, 20% at 120 °C and 99% at 160 °C. Even the boiling point (337 °C) of sulfuric acid is higher than the desolvation temperature of 160 °C, the dilute sulfate concentration cannot be preserved at temperatures >120 °C. The sulfur loss can be attributed to the formation of an azeotrope between the remaining nitric acid (solvent) and sulfuric acid (solute) above 122 °C, the boiling point of 68% nitric acid. With the addition of sodium, sulfur can be conserved. This observation suggests that the formation of sodium sulfate suppresses sulfur vaporization.

3.3. Transmission of sulfur through membrane desolvation

Determinations of sulfur with and without sodium addition through membrane desolvation are plotted in Fig. 2. Without the addition of sodium, the sulfur is only 1.2% in the plasma, 6.7% in the gas, and 0.1% in the wash out. Most of the lost sulfur is retained on the desolvation membrane. The retained sulfur can be gradually released during a 30-min injection of 0.25 mol L^{-1} HNO_3 with the addition of sodium, about 10% of which flows to the plasma and 82% to the gas waste. With the addition of sodium, 98% of sulfur is successfully delivered to the plasma.

The desolvation temperature effect for sulfur vaporization is plotted in Fig. 3. Without sodium additive, the ion beam intensity of $^{32}S^{+}$ decreases dramatically from 1 V at 70 °C to 0.1 V at 90 °C, and even down to the background level at temperatures >110 °C. For the solution doped with sodium, the sulfur signal elevates gradually with increasing temperature and approaches 10 V when temperature reaches 150–160 °C.

Our tests clearly show sulfur adsorption onto the hydrophobic PTFE membrane. Sulfur, with the form of sodium sulfate, can be carried to the plasma by adding an appropriate amount of cation solution.

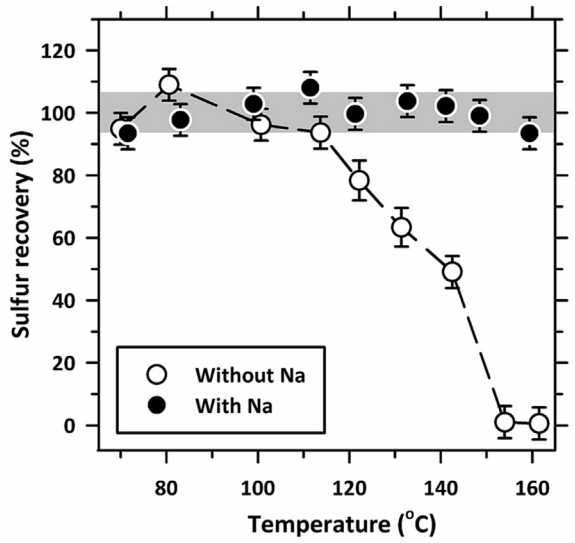

Fig. 1. Effect of sodium on changing sulfur volatility. Sulfur loss evaluation with and without sodium addition with temperature varying from 70 to 160 °C. Gray area shows the acceptable sulfur recovery range.

3.4. Sulfur isotopic analysis with sodium additive

The addition of several different cations has been shown to overcome desolvation-induced sulfur losses, including sodium [25], silver [26] and ammonium [27]. By using silver or ammonium, the formation of insoluble AgCl or NH_4Cl may clog the membrane if chloride is not entirely removed before instrumental analysis. Sodium appears to be an ideal choice. Moreover, the use of Na-doped HNO_3 (i.e., 0.31 μmol L^{-1} Na) provides a validated sign for real blank monitoring, which is important when background subtraction is involved in sulfur isotope ratio calculation.

Evaluation of an appropriate amount of sodium addition is plotted in Fig. 4. At Na/S < 2, the sulfur intensity increases with increasing Na/S ratio. The maximal ion beam intensity (Fig. 4A) and stable isotope ratios (Fig. 4B) can be achieved when Na/S mole ratio is 2 or higher. The optimal Na/S ratio of 2 may reflect the molar stoichiometric proportion of Na_2SO_4. Sulfur signal enhancement reaches the plateau at Na/S ratios >1, implying the possible formation of $NaHSO_4$ (~50% SO_4^{2-} would convert to HSO_4^{-} at pH 2). Good external precision of 22.60 ± 0.19‰ for the ^{34}S measurement can be offered under the conditions with a Na/S ratio ≧2. Our results show that the amount of sodium additive can be operationally fixed at a Na/S mole ratio of 2 for high precision sulfur isotopic measurements.

3.5. Precision and accuracy, and reproducibility

Analytical performance was determined by running the ICP-MS working standard SPEX-S solution over a 3-year course, from 2014 to 2017 (Fig. 5). Within-run precision (2 SD) is ±0.14‰ for $^{33}S/^{32}S$ and ±0.20‰ for $^{34}S/^{32}S$ at 0.1 nmol S (i.e., 3.2 ng S in 1 mL solution), and ±0.005‰ and ±0.015‰, respectively, at 9 nmol S (i.e., 288 ng S in 1 mL solution). High precision analysis can be achieved for $\delta^{34}S$ at ^{32}S intensities higher than 2.5 V (0.8 μmol L^{-1} S), and at ^{32}S intensities above 6.5 V (2 μmol L^{-1} S) for $\Delta^{33}S$ (Fig. 5A and B), resulting in between-run uncertainties (2 SD) of ±0.39‰ for $\delta^{34}S$ and ±0.20‰ for $\Delta^{33}S$. Results show that our methodology can produce precise and accurate S isotopic measurements using 3 nmol S for $\Delta^{33}S$. The long-term precision is ±0.18‰ for $\delta^{34}S$ and ±0.10‰ for $\Delta^{33}S$ (Fig. 5C and D). The $\delta^{34}S$ values of measured standard reference materials, IAEA-S-2, IAEA-S-3, and NASS-5, are 22.60 ± 0.19‰, −32.12 ± 0.18‰ and 21.53 ± 0.15‰, respectively. These values agree with previously reported data (Table 2). Replicate analyses of one Ag_2S sample is shown in Table 2. Its $\Delta^{33}S$ is determined to be −0.81 ± 0.12‰, consistent with previously analyzed values measured by Isotope Ratio Mass Spectrometer [30,31]. This consistency supports the fidelity of our methodology.

3.6. Sulfur isotopic compositions in marine pore-fluids

The pore fluid sulfate concentrations and sulfur isotopic compositions are shown in Fig. 6. Sulfate decreases from 27.6 at the sea surface to 0.4 mmol L^{-1} at the deepest depth of 232 cm below seafloor (cmbsf). Depth profiles of $\delta^{34}S$ and $\Delta^{33}S$ were measured with 3–6 nmol S increases from 21.5 to 26.1‰ at depths of 0–152.5 cmbsf, which might be attributed to sulfate consumption by the degradation of organic matter [8]. At depths >152.5 cmbsf, rapid consumption of sulfate occurs through AOM coupled with sulfate reduction [7,8], resulting in sulfate depletion and elevated $\delta^{34}S$ approaching 54.3‰ at the sulfate methane transition zone, a depth of 212.5 cmbsf. $\delta^{34}S$ value at the deepest depth of 232 cmbsf is 34.0‰, resulting from a binary mixing of remaining sulfate (54.3‰) and hydrogen sulfide (HS^{-}) (20‰) [38]. This indicates that the 0.4 mmol L^{-1} sulfate at this depth is a mixture of sulfate in

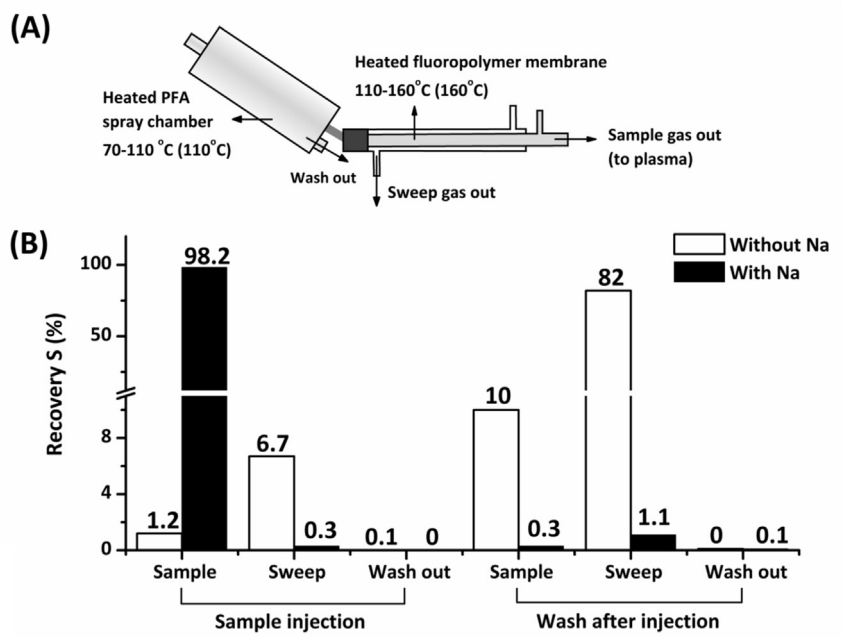

Fig. 2. **(A)** Schematic of a desolvation device ARIDUS I, made of PFA spray chamber (width 4.5 cm and length 14 cm) and fluoropolymer membrane (length ~2.4 m). Three outflow routes include sample gas out to plasma, sweep gas out and waste out from spray chamber to drain. **(B)** Proportion of sulfur collected from different outflow loops after a 30-min introduction of sulfur and with or without sodium.

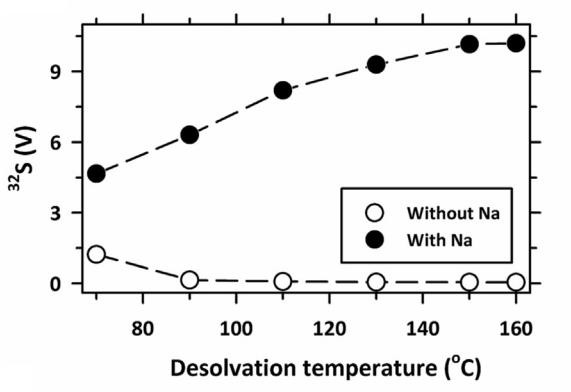

Fig. 3. Comparison between sulfur intensity and desolvation temperature with (solid circles) or without (hollow cricles) sodium addition. The concentration of sulfur is 3 μmol L^{-1} (i.e., 100 μg L^{-1}).

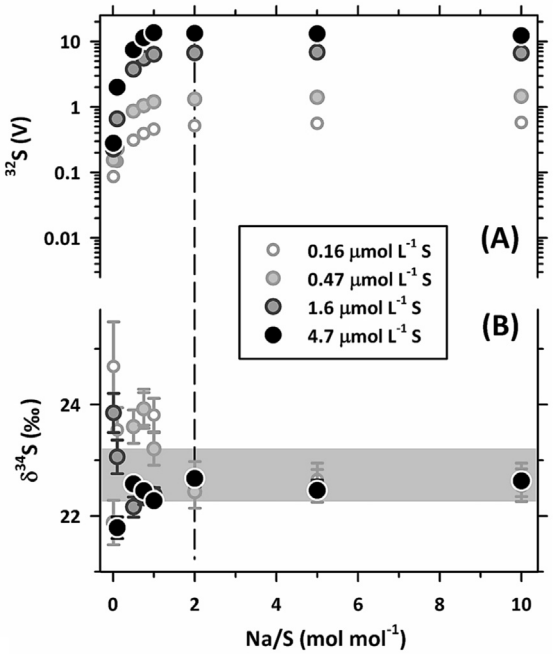

Fig. 4. Changes of **(A)** sulfur intensity and **(B)** $\delta^{34}S$ with various amount of sodium added (desolvation temperature at 160 °C). Sulfur concentration ranges from 0.16 to 4.7 μmol L^{-1} and Na/S molar ratios from 0.01 to 10. Dashed line denotes a Na/S molar ratio of 2. Gray areas denote the acceptable ranges (average ± 2 SD, compiled from the reported values in Table S5).

remaining pore fluid and hydrogen sulfide that was reoxidized during pore fluid collection. $\Delta^{33}S$ shows a constant value of −0.05 ± 0.08‰, implying that sulfate-reducing bacteria did not play a significant role in the mass independent sulfur signal [39].

4. Conclusions

We carefully evaluated and improved the transmission of sulfur via desolvation for high-precision sulfur isotopic analysis on an MC-ICP-MS. We quantitatively overcame the serious sulfur loss (~99%) in membrane desolvation apparatus by adding an appropriate amount of sodium. The addition of sodium to wash solution is also essential for memory reduction and instrumental blank monitoring. Our simple mini-column purification techniques achieve high sulfur recovery yield of >97% and low S blank of 19 pmol, benefiting for precise $\delta^{34}S$ and $\Delta^{33}S$ analyses with small sample requirement of 3 nmol sulfur. Two-sigma reproducibility is ±0.18‰ for $\delta^{34}S$ and ±0.10‰ for $\Delta^{33}S$. The robust techniques are successfully applied to low-sulfur pore fluids for studying microbial sulfur reduction-methane oxidation in marginal sea sediments. For offshore southwestern Taiwan, further measurements in different cores drilled at various environments in this area, including cold seeps and mud volcanoes, are required to fully understand the

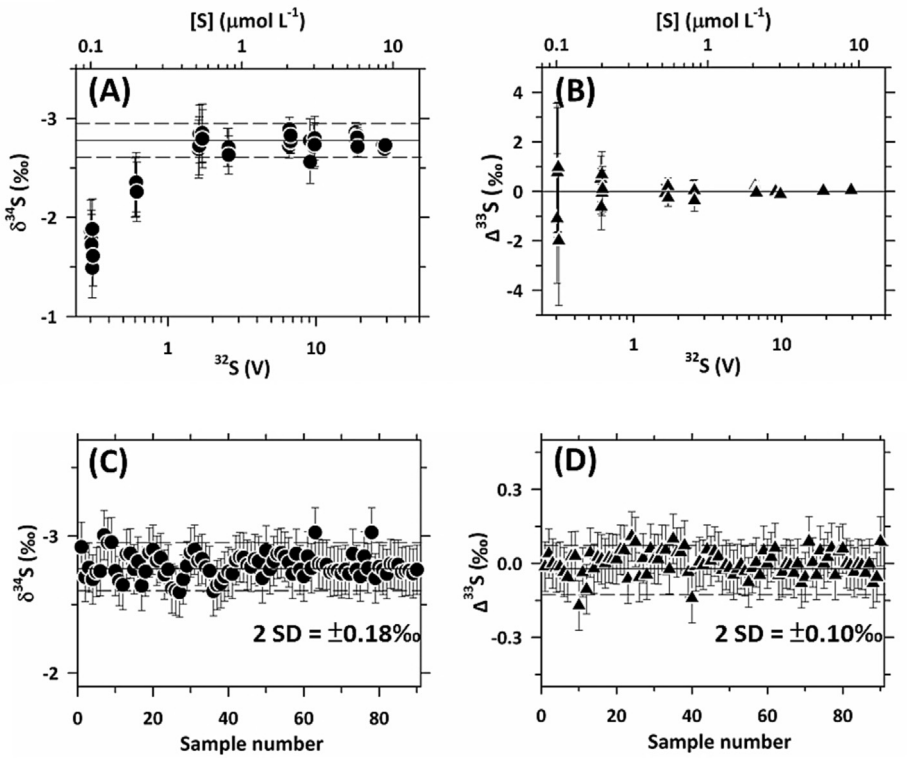

Fig. 5. Measurement of **(A)** $\delta^{34}S$ and **(B)** $\Delta^{33}S$ on aliquots with ^{32}S ion beam intensities of 0.3–29 V for in-house ICP-MS working standard SPEX-S solution. Three-year reproducibility of **(C)** $\delta^{34}S$ and **(D)** $\Delta^{33}S$ with 3 nmol S for working standard SPEX-S. Dashed lines denote the overall external 2-sigma ranges.

Table 2
MC-ICP-MS results for reference materials and working standards.

Name	Sample type	$\delta^{33}S_{IAEA-S-1}$ (‰)	2 SD	$\delta^{34}S_{IAEA-S-1}$ (‰)	2 SD	$\Delta^{33}S$ (‰)	2 SD	n
IAEA-S-2	Synthetic Ag_2S	11.46	0.19	22.60	0.19	−0.11	0.11	7
References compiled[a]		**11.52**	**0.30**	**22.73**	**0.47**	**−0.06**	**0.24**	
IAEA-S-3	Synthetic Ag_2S	−16.68	0.14	−32.12	0.18	0.01	0.10	9
References compiled[a]		**−16.61**	**0.17**	**−32.11**	**0.50**	**0.04**	**0.34**	
NASS-5	Seawater	10.97	0.14	21.53	0.15	−0.05	0.11	9
References compiled[a,b]		**11.04**	**0.17**	**21.41**	**0.37**	**0.06**	**0.03**	
PPRG0486	Ag_2S	0.10	0.14	1.80	0.17	−0.81	0.12	3
Reference value [30,31]		**0.35**	**0.40**	**1.63**	**0.40**	**−0.69**	**0.07**	**3**
HP-S	Sulfur in H_2O	4.73	0.10	9.24	0.15	−0.02	0.07	15
SPEX-S	Sulfur in H_2O	−1.46	0.14	−2.78	0.18	−0.03	0.10	90

[a] The compiled data are the mean and 2 SD of the previous reported values (Table S5).
[b] Assuming a constant seawater S isotopic composition.

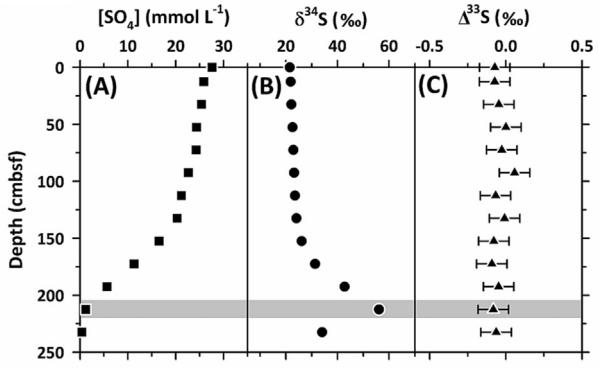

Fig. 6. Depth profiles of marine sediment pore fluid **(A)** dissolved sulfate concentration, **(B)** $\delta^{34}S$, and **(C)** $\Delta^{33}S$ at 0–240 cm depth below the seafloor (cmbsf). Gray area indicates the sulfate-methane transition zone (SMTZ).

microbial roles of sulfur isotopic fractionation at and below the SMTZ.

Acknowledgements

We greatly thank Nai-Chen Chen and Chun-Yuan Huang for their assistance on pore water collection and analysis, and Hsuan-Wen Chen for his assistance on desolvation membrane sulfur recovery experiment. The study was financially supported by grants from Taiwan ROC MOST (104-2119-M-002-003, 105-2119-M-002-001 to C.-C.S. and 103-2116-M-002-027-MY3 to Y.-G.C.) and National Taiwan University (105R7625 to C.-C.S.).

Appendix A. Supplementary data

Supplementary data related to this article can be found at http://dx.doi.org/10.1016/j.aca.2017.08.012.

References

[1] S.H. Bottrell, R.J. Newton, Reconstruction of changes in global sulfur cycling from marine sulfate isotopes, Earth-Sci Rev. 75 (2006) 59–83.

[2] P. Brimblecombe, The Global Sulfur Cycle, Treatise on Geochemistry, Elsevier, 2003.

[3] D.T. Johnston, Multiple sulfur isotopes and the evolution of Earth's surface sulfur cycle, Earth-Sci Rev. 106 (2011) 161–183.

[4] M. Fontecave, Iron-sulfur clusters: ever-expanding roles, Nat. Chem. Biol. 2 (2006) 171–174.

[5] M. Giordano, A. Norici, R. Hell, Sulfur and phytoplankton: acquisition, metabolism and impact on the environment, New Phytol. 166 (2005) 371–382.

[6] D.A. Fike, A.S. Bradley, C.V. Rose, Rethinking the ancient sulfur cycle, Annu. Rev. Earth Pl. Sc 43 (2015) 593–622.

[7] P. Aharon, B.S. Fu, Microbial sulfate reduction rates and sulfur and oxygen isotope fractionations at oil and gas seeps in deepwater Gulf of Mexico, Geochim. Cosmochim. Ac 64 (2000) 233–246.

[8] G. Antler, A.V. Turchyn, B. Herut, A. Davies, V.C.F. Rennie, O. Sivan, Sulfur and oxygen isotope tracing of sulfate driven anaerobic methane oxidation in estuarine sediments, Estuar. Coast Shelf S 142 (2014) 4–11.

[9] C. Deusner, T. Holler, G.L. Arnold, S.M. Bernasconi, M.J. Formolo, B. Brunner, Sulfur and oxygen isotope fractionation during sulfate reduction coupled to anaerobic oxidation of methane is dependent on methane concentration, Earth Planet Sc Lett. 399 (2014) 61–73.

[10] T. Treude, S. Krause, J. Maltby, A.W. Dale, R. Coffin, L.J. Hamdan, Sulfate reduction and methane oxidation activity below the sulfate-methane transition zone in Alaskan Beaufort Sea continental margin sediments: implications for deep sulfur cycling, Geochim. Cosmochim. Ac 144 (2014) 217–237.

[11] L. Holmkvist, T.G. Ferdelman, B.B. Jorgensen, A cryptic sulfur cycle driven by iron in the methane zone of marine sediment (Aarhus Bay, Denmark), Geochim. Cosmochim. Ac 75 (2011) 3581–3599.

[12] H.G. Thode, J. Monster, H.B. Dunford, Sulphur isotope geochemistry, Geochim. Cosmochim. Ac 25 (1961) 159–174.

[13] C.E. Rees, Sulfur isotope measurements using SO_2 and SF_6, Geochim. Cosmochim. Ac 42 (1978) 383–389.

[14] A. Giesemann, H.J. Jager, A.L. Norman, H.P. Krouse, W.A. Brand, Online sulfur-isotope determination using an elemental analyzer coupled to a mass-spectrometer, Anal. Chem. 66 (1994) 2816–2819.

[15] J.L. Mann, W.R. Kelly, Measurement of sulfur isotope composition ($\delta^{34}S$) by multiple-collector thermal ionization mass spectrometry using a ^{33}S-^{36}S double spike, Rapid Commun. Mass Sp. 19 (2005) 3429–3441.

[16] L.R. Riciputi, D.R. Cole, H.G. Machel, Sulfide formation in reservoir carbonates of the Devonian Nisku Formation, Alberta, Canada: an ion microprobe study, Geochim. Cosmochim. Ac 60 (1996) 325–336.

[17] E.H. Hauri, D. Papineau, J.H. Wang, F. Hillion, High-precision analysis of multiple sulfur isotopes using NanoSIMS, Chem. Geol. 420 (2016) 148–161.

[18] T. Prohaska, C. Latkoczy, G. Stingeder, Precise sulfur isotope ratio measurements in trace concentration of sulfur by inductively coupled plasma double focusing sector field mass spectrometry, J. Anal. At. Spectrom. 14 (1999) 1501–1504.

[19] A. Amrani, A.L. Sessions, J.F. Adkins, Compound-specific $\delta^{34}S$ analysis of volatile organics by coupled GC/multicollector-ICPMS, Anal. Chem. 81 (2009) 9027–9034.

[20] R. Clough, P. Evans, T. Catterick, E.H. Evans, $\delta^{34}S$ measurements of sulfur by multicollector inductively coupled plasma mass spectrometry, Anal. Chem. 78 (2006) 6126–6132.

[21] P.R. Craddock, O.J. Rouxel, L.A. Ball, W. Bach, Sulfur isotope measurement of sulfate and sulfide by high-resolution MC-ICP-MS, Chem. Geol. 253 (2008) 102–113.

[22] P.R.D. Mason, J. Kosler, J.C.M. de Hoog, P.J. Sylvester, S. Meffan-Main, In situ determination of sulfur isotopes in sulfur-rich materials by laser ablation multiple-collector inductively coupled plasma mass spectrometry (LA-MC-ICP-MS), J. Anal. At. Spectrom. 21 (2006) 177–186.

[23] A. Das, C.H. Chung, C.F. You, M.L. Shen, Application of an improved ion exchange technique for the measurement of $\delta^{34}S$ values from microgram quantities of sulfur by MC-ICPMS, J. Anal. At. Spectrom. 27 (2012) 2088–2093.

[24] P.R.D. Mason, K. Kaspers, M.J. van Bergen, Determination of sulfur isotope ratios and concentrations in water samples using ICP-MS incorporating hexapole ion optics, J. Anal. At. Spectrom. 14 (1999) 1067–1074.

[25] G. Paris, A.L. Sessions, A.V. Subhas, J.F. Adkins, MC-ICP-MS measurement of $\delta^{34}S$ and $\Delta^{33}S$ in small amounts of dissolved sulfate, Chem. Geol. 345 (2013) 50–61.

[26] S.H. Han, Z. Varga, J. Krajko, M. Wallenius, K. Song, K. Mayer, Measurement of the sulphur isotope ratio ($^{34}S/^{32}S$) in uranium ore concentrates (yellow cakes) for origin assessment, J. Anal. At. Spectrom. 28 (2013) 1919–1925.

[27] E. Albalat, P. Telouk, V. Balter, T. Fujii, V.P. Bondanese, M.L. Plissonnier, V. Vlaeminck-Guillem, J. Baccheta, N. Thiam, P. Miossec, F. Zoulim, A. Puisieux, F. Albarede, Sulfur isotope analysis by MC-ICP-MS and application to small medical samples, J. Anal. At. Spectrom. 31 (2016) 1002–1011.

[28] O. Hanousek, M. Brunner, D. Profrock, J. Irrgeher, T. Prohaska, The performance of single and multi-collector ICP-MS instruments for fast and reliable $^{34}S/^{32}S$ isotope ratio measurements, Anal. Methods-Uk 8 (2016) 7661–7672.

[29] C.-C. Shen, K.-S. Li, K. Sieh, D. Natawidjaja, H. Cheng, X. Wang, R.L. Edwards, D.D. Lam, Y.-T. Hsieh, T.-Y. Fan, A.J. Meltzner, F.W. Taylor, T.M. Quinn, H.-W. Chiang, K.H. Kilbourne, Variation of initial $^{230}Th/^{232}Th$ and limits of high precision U-Th dating of shallow-water corals, Geochim. Cosmochim. Ac 72 (2008) 4201–4223.

[30] G.X. Hu, D. Rumble, P.-L. Wang, An ultraviolet laser microprobe for the in situ analysis of multisulfur isotopes and its use in measuring Archean sulfur isotope mass-independent anomalies, Geochim. Cosmochim. Ac 67 (2003) 3101–3118.

[31] J. Farquhar, H.M. Bao, M. Thiemens, Atmospheric influence of Earth's earliest sulfur cycle, Science 289 (2000) 756–758.

[32] N.-C. Chen, T.-F. Yang, W.-L. Hong, H.-W. Chen, H.-C. Chen, C.-Y. Hu, Y.-C. Huang, S. Lin, L.-H. Lin, C.-C. Su, W.-Z. Liao, C.-H. Sun, P.-L. Wang, T. Yang, S.-Y. Jiang, C.-S. Liu, Y. Wang, S.-H. Chung, Production, consumption, and migration of methane in accretionary prism of southwestern Taiwan, Geochem. Geophys. Geosy. 18 (2017), http://dx.doi.org/10.1002/2017GC006798.

[33] A.A. Menegario, M.F. Gine, J.A. Bendassolli, A.C.S. Bellato, P.C.O. Trivelin, Sulfur isotope ratio ($^{34}S/^{32}S$) measurements in plant material by inductively coupled plasma mass spectrometry, J. Anal. At. Spectrom. 13 (1998) 1065–1067.

[34] B.-S. Wang, C.-F. You, K.-F. Huang, S.-F. Wu, S.K. Aggarwal, C.-H. Chung, P.-Y. Lin, Direct separation of boron from Na- and Ca-rich matrices by sublimation for stable isotope measurement by MC-ICP-MS, Talanta 82 (2010) 1378–1384.

[35] J. Farquhar, B.A. Wing, Multiple sulfur isotopes and the evolution of the atmosphere, Earth Planet Sc Lett. 213 (2003) 1–13.

[36] S. Ono, B. Wing, D. Rumble, J. Farquhar, High precision analysis of all four stable isotopes of sulfur (^{32}S, ^{33}S, ^{34}S and ^{36}S) at nanomole levels using a laser fluorination isotope-ratio-monitoring gas chromatography-mass spectrometry, Chem. Geol. 225 (2006) 30–39.

[37] J.R. Hulston, H.G. Thode, Variations in S^{33}, S^{34} and S^{36} contents of meteorites and their relation to chemical and nuclear effects, J. Geophys Res. 70 (1965) 3475–3484.

[38] B. Brunner, G.L. Arnold, H. Roy, I.A. Muller, B.B. Jorgensen, Off limits: sulfate below the sulfate methane transition, Front. Earth Sci. 4 (2016), http://dx.doi.org/10.3389/feart.2016.00075.

[39] I. Halevy, D.T. Johnston, D.P. Schrag, Explaining the structure of the archean mass-independent sulfur isotope record, Science 329 (2010) 204–207.